

friction and heat flux at the stagnation point of a concave obstacle, using relations for a two-dimensional flat plate, accounting for variation in the velocity gradient at the stagnation point of the obstacle, gives underestimated values (by a factor from 3 to 8), compared with the present results.

NOTATION

ξ, ζ , axes of the body-fixed coordinate system; ξ_∞ , distance from the obstacle at which the effect of the obstacle and the outer flow is negligibly small; x, y , rectangular coordinate system axes; y_∞ , thickness of viscous layer on the obstacle; y_T , coordinate of the obstacle surface; η , transformed coordinate; t , time; φ , slope angle of the velocity vector V_∞ to the axis of symmetry; u, v , velocity components along the axes ξ, ζ in the region of interaction of an ideal flow with the obstacle; U, V , velocity components along the x and y axes in the obstacle boundary layer; V_∞ , velocity at section ξ_∞ ; U_1 , gradient of U in direction x ; β , velocity gradient at the obstacle stagnation point; ρ , density; T , temperature; T_w , wall temperature; T_∞ , temperature of outer flow; p , pressure; μ , dynamic viscosity; λ , thermal conductivity; c_p , specific heat; α , heat-transfer coefficient; K , curvature of obstacle; τ_w , friction on the obstacle surface; q_w , heat flux to the obstacle surface; Q, H , sizes of computational mesh cell in the direction of the x and η axes, respectively; Δt , time step; i, j, m , cell numbers in the directions x, η , and t ; k , iteration number; w , relaxation coefficient; $Re = \rho V_\infty \xi_\infty / \mu$, Reynolds number; $Pr = c_p \mu / \lambda$, Prandtl number; $Ec = \sqrt{V_\infty^2 (c_p T_\infty)}$, Eckert number; $Nu = \alpha \xi_\infty / \lambda$, Nusselt numbers. Indices: 0, parameters at the outer edge of the boundary layer; f.p., parameters on a two-dimensional flat plate, positioned normal to a uniform external stream; -, dimensional value.

LITERATURE CITED

1. V. M. Paskonov, in: Some Applications of the Mesh Method, No. 1 Boundary-Layer Flows [in Russian], Izd. MGU (1971).
2. C. L. S. Farn and V. S. Arpaci, AIAA J., 4, 730 (1966).
3. I. P. Ginzburg, Theory of Hydraulic Resistance and Heat Transfer [in Russian] Izd. LGU (1970).

MECHANISM OF BOILING ON SUBMERGED SURFACES WITH CAPILLARY-POROUS COATING

O. N. Man'kovskii, O. B. Ioffe,
L. G. Fridgart, and A. R. Tolchinskii

UDC 536.423.1

An approximate model is proposed for the process of boiling in a porous layer. The model shows satisfactory qualitative and quantitative agreement with experimental data over a wide range of heat fluxes.

Heat-transfer surfaces with capillary-porous coatings have been arousing much interest among researchers, since boiling seems to occur on them somewhat more intensely than on uncoated surfaces. In particular, it has been noticed that boiling on porous surfaces may occur for very small temperature differences, hence permitting the transfer of large heat fluxes in thermodynamically favorable conditions.

The study of this phenomenon is known to present certain difficulties, since its mechanism is determined by heat-transfer processes that occur inside the structure of the capillary-porous layer, where they are inaccessible to visual observation and direct measurement. Probably as a result, the literature has so far lacked any general methods allowing the calculation and analysis of this process on the basis of specified properties of the medium, parameters of the porous layer, the characteristics of the coating material, and the temperature difference. Experimental results and empirical correlations were presented in [1-3],

Translated from *Inzhenerno-Fizicheskii Zhurnal*, Vol. 30, No. 2, pp. 310-316, February, 1976. Original article submitted December 2, 1974.

This material is protected by copyright registered in the name of Plenum Publishing Corporation, 227 West 17th Street, New York, N.Y. 10011. No part of this publication may be reproduced, stored in a retrieval system, or transmitted, in any form or by any means, electronic, mechanical, photocopying, microfilming, recording or otherwise, without written permission of the publisher. A copy of this article is available from the publisher for \$7.50.

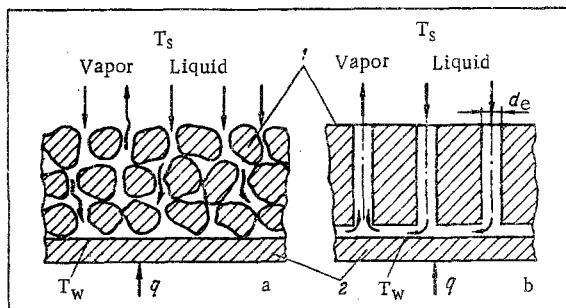


Fig. 1. Structure of porous surface: a) actual; b) model representation; 1) porous layer; 2) supporting surface.

but these cannot be extended to cases that differ significantly from the conditions of the experiments in which they were obtained.

In the present work, an attempt is made to construct a simplified mathematical model based on physical ideas as to the most significant aspects of the process. If the experimental results for boiling in porous coatings [1, 2, 4] are analyzed, the following information on the mechanism of the process is obtained. When a liquid is heated inside a porous layer, vapor is formed and drawn off through certain pores, while through other pores, on account of the action of capillary forces, new portions of liquid are drawn into the layer (Fig. 1a). What exactly is it that allows high thermal fluxes to be obtained and also developed bubble boiling to occur at such a low ΔT (fractions of a degree), when boiling on surfaces that have no porous coating requires far greater superheating before vapor bubbles will form and grow? One explanation is to assume that inside the porous layer there are cavities containing phase boundaries. Since these cavities are large in comparison with ordinary newly formed vapor bubbles, vaporization will occur for incomparably smaller superheating in these cavities than in the interior of a vapor bubble. Liquid drawn into the layer by capillary forces is heated by contact with the granules forming the porous structure, which have a higher temperature than the liquid on account of their significant thermal conductivity. We estimate the intensity of this heat transfer.

The liquid motion in the capillary channels may be assumed to be laminar. For small Reynolds number, the heat-transfer coefficient for laminar flow may be determined from the equation [6]

$$\alpha = C \frac{\lambda_L}{d_h}, \quad (1)$$

where C is a constant depending on the channel geometry; for a circular channel cross section, $C = 3.65$. Since channel diameters in the capillary-porous layer are of the order of 10^{-3} - 10^{-5} m, the heat-transfer coefficient will be of order 10^3 - 10^5 W/(m²·deg). In addition, the heat-transfer surface is highly developed.

Thus, the high heat fluxes at small temperature differences in boiling in porous surfaces may be explained by three factors:

- 1) the presence inside the layer of phase boundaries, reducing the heating necessary for vapor formation;
- 2) the high convective heat-transfer coefficient for laminar motion of a liquid in a capillary channel;
- 3) the developed surface of the capillary structure.

On the basis of the proposed mechanism for the phenomenon, a porous layer may be approximately represented as a system of communicating capillaries (Fig. 1b). So as to simplify the geometry, we assume that the channels are circular. The hypothetical capillary layer should be equivalent to the real porous layer in three fundamental respects: hydrodynamically, thermally, and in terms of capillary uplift. In order to characterize the capillaries in relation to these properties, we will use three diameters: d_c to describe the capillary effect; d_h , the equivalent hydraulic diameter; and d_t , the equivalent thermal diameter.

According to [7], the capillary effect in the case of a wet layer can be described by the value

$$d_c = 0.41 d. \quad (2)$$

According to [8], the equivalent hydraulic diameter is

$$d_h = \frac{1}{3} \cdot \frac{\varepsilon d}{1 - \varepsilon}, \quad (3)$$

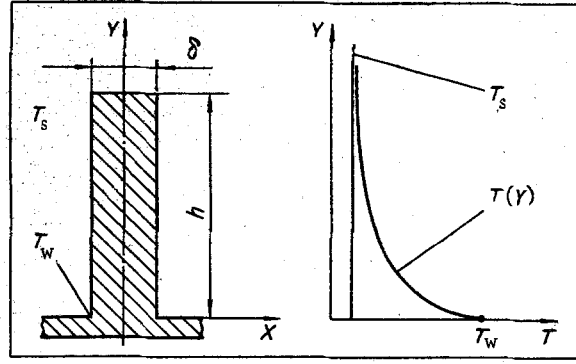


Fig. 2. Temperature profile in the wall of the equivalent capillary.

where ϵ is the porosity (ratio of the volume of the cavities to the volume of the layer).

The equivalent thermal diameter is determined from the condition that the capillaries and the pores must have the same volume and surface,

$$d_t = \frac{2}{3} \frac{\epsilon d}{1 - \epsilon} = 2d_h \quad (4)$$

The capillary wall thickness δ can be determined from the equality of the volume of the granules to the volume of the capillary walls:

$$\delta = \frac{d_t}{2} \left(\sqrt{\frac{1}{\epsilon}} - 1 \right) = \frac{\epsilon}{3(1 - \epsilon)} \left(\sqrt{\frac{1}{\epsilon}} - 1 \right) d. \quad (5)$$

Assume that, in stable conditions, one vapor-discharge capillary connects with m liquid (vapor-generating) capillaries. The most probable position of the phase boundary would be close to the heated surface, since it is here that conditions are particularly favorable for vapor formation. Thus, one center of vapor formation is made up of $(m + 1)$ capillaries, m of which are filled with liquid over the whole depth h . We assume that heat transfer in the vapor-discharge capillary is negligibly small. If q_c is the heat-flux density in the vapor-generating capillary, then the amount of heat arriving at one vapor-formation center is

$$Q = \pi d_h h q_c m. \quad (6)$$

The heat-flux density referred to the smooth surface is

$$q = QM = \pi d_t h q_c m \frac{n}{m + 1} = \frac{24(1 - \epsilon)h}{d} q_c \frac{m}{m + 1}, \quad (7)$$

where $M = n/(m + 1)$ is the number of vapor-formation centers per unit area; $n = 4\epsilon/\pi d_h^2$ is the number of capillaries per unit area.

If we neglect inertial forces, stresses, and surface tension in the formation of bubbles above the liquid surface, the pressure difference arising on account of capillary forces is equal to the resistance to vapor and liquid motion in the capillaries:

$$\Delta P_c = \Delta P_V + \Delta P_L. \quad (8)$$

Assuming that liquid and vapor motion in the capillaries is laminar, we may calculate the pressure difference by means of Poiseuille's formula,

$$\Delta P_L = \frac{128\mu_L h}{\pi d_h^4 \rho_L} G_L, \quad (9)$$

$$\Delta P_V = \frac{128\mu_V h}{\pi d_h^4 \rho_V} G_V m. \quad (10)$$

The pressure difference due to capillary forces may be calculated from the well-known relation

$$\Delta P_c = \frac{4\sigma \cos \theta}{d_c}. \quad (11)$$

Substituting Eqs. (9), (10), and (11) into Eq. (8), and bearing in mind that

$$G_L = \frac{\pi d_h h q_c}{r}, \quad (12)$$

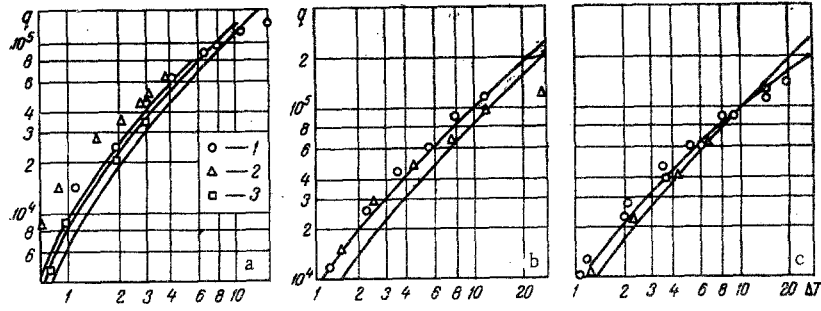


Fig. 3. Comparison of results given by Eq. (19) with the experimental data of [2]: a) $d = 0.359$ mm; 1) $h = 3.15$ mm; 2) 12.7; 3) 25.4; b) $d = 0.507$ mm; 1) $h = 3.15$ mm; 2) 25.4; c) $d = 0.507$ mm; 1) $h = 12.7$ mm; 2) 38.1. q , W/m^2 ; ΔT , $^{\circ}K$.

we find the expression

$$m = 1.41 \cdot 10^{-3} \frac{\sigma r \rho_V \cos \theta}{\mu_V q_c} \left(\frac{d}{h} \right)^2 \left(\frac{\varepsilon}{1 - \varepsilon} \right)^3 - \Delta m, \quad (13)$$

where $\Delta m = \mu_{LPV} / \mu_{VPL}$.

To determine the heat flux in the capillary q_c , we regard its wall, in the first approximation, as a rectangular fin of height h , length $\pi d h$, and thickness δ , having a thermal conductivity equal to that of a porous layer in vacuo λ_l (Fig. 2). We will assume that the temperature of the liquid surrounding the fin is constant over the height and equal to the saturation temperature at the pressure calculated taking into account the curvature of the meniscus in the capillary. It is known [9] that, if T_s is the saturation temperature in the volume of the liquid, then the superheating due to the curvature of the meniscus (nucleational superheating) is given approximately by

$$\Delta T^* = \frac{4\sigma T_s}{r \rho_V d_c} = 9.75 \frac{\sigma T_s}{r \rho_V d}. \quad (14)$$

The temperature difference at the base of the fin is

$$\Delta T_b = (T_w - T_s) - \Delta T^* = \Delta T - \Delta T^*. \quad (15)$$

For the given assumptions, the heat flux per unit length of the fin base is [10]

$$Q_c = \delta \lambda_l \left(\frac{2\alpha}{\delta \lambda_l} \right)^{0.5} \Delta T_b \operatorname{th} \left(h \sqrt{\frac{2\alpha}{\delta \lambda_l}} \right). \quad (16)$$

In Eq. (16) the hyperbolic tangent may be assumed equal to unity since, under the conditions of the considered problem, its argument is large. Referring the heat flux to the surface area of the capillary, we have

$$q_c = \frac{\delta}{h} \lambda_l \sqrt{\frac{2\alpha}{\delta \lambda_l}} \Delta T_b. \quad (17)$$

We calculate α from Eq. (1) and, after elementary transformations, we obtain

$$q_c = \frac{2.7}{h} \left[\left(\sqrt{\frac{1}{\varepsilon}} - 1 \right) \lambda_L \lambda_l \right]^{0.5} (\Delta T - \Delta T^*). \quad (18)$$

Substituting Eq. (18) into Eq. (7) leads finally to

$$q = \frac{64.8(1 - \varepsilon)}{d} \left[\left(\sqrt{\frac{1}{\varepsilon}} - 1 \right) \lambda_L \lambda_l \right]^{0.5} (\Delta T - \Delta T^*) \frac{m}{m + 1}, \quad (19)$$

where m can be calculated from Eqs. (13) and (17).

Comparing Eq. (19) with the experimental data of [2] gives the results shown in Fig. 3. As is evident, the model provides satisfactory agreement with the results of all the available series of experiments in a wide range of heat fluxes. The general trends predicted by the model for the dependence of the heat-flux density on all the parameters varied in the experiments are qualitatively correct. Thus, the dependence of q on ΔT is linear for $m \gg 1$, i.e., far from the critical region. The empirical correlation given in [2] for the experimental results obtained there practically coincides in shape with Eq. (19).

Likewise, qualitative comparisons showed the proposed model to be consistent with the experimental data of [1, 11, 12] (no quantitative treatment was carried out, since the necessary characteristics were not available). In all cases, the experimental data can be described, with a certain accuracy, by a linear dependence of q on ΔT . The equations given in [11] also show the same behavior. The only exception is the nearly quadratic dependence of q on ΔT obtained in [3], where the dependence of α on ΔT was found to be close to linear. An analysis in [3] of the data obtained in [2] revealed a certain nonlinearity of the dependence $\log q = f(\log \Delta T)$, which is, in fact, clearly visible at low values of ΔT , and a dependence of α on q , whereas in [2] it was assumed that $\alpha = \text{const}$.

Equation (19) explains this phenomenon as the effect of nucleational superheating ΔT^* , which for the experimental conditions of [2], for example, for $d = 0.5$ mm, is equal to 0.3°K . In this case, at small values of ΔT , it should be assumed that the dependence of q on ΔT has the form $q = A\Delta T + C$ [see Eq. (19)] and is not linear in logarithmic coordinates.

Thus, although the curvature of the initial portion of $\log q = f(\log \Delta T)$ indicates the effect of the heat flux on α , this does not disprove the linear character of the dependence of q on ΔT and does not allow the experimental results of [3] to be explained. Evidently, the experimental data of [3] must refer to a phenomenon which is qualitatively different from that observed in the other works. It is unlikely that the difference in the results of [3] and [2] can be explained by the different heat conductivities of the layer materials, since experiments on a layer of glass balls [1] gave a qualitative picture analogous to that obtained on Monel balls [2]. It may be assumed that the process under consideration is affected by the ratio of the channel diameter to the breakaway diameter of the vapor bubbles, since this ratio was significantly larger in [3] than in [2].

Thus, there are sufficient grounds to assume that Eq. (19) correctly describes the effect of ΔT on q , despite the existence of experiments that disagree with it.

The effects of the other parameters predicted by the model are qualitatively correct and agree with the available experimental data. Thus, experimentally (except for [3]) and in Eq. (19), an inverse dependence on the granule diameter is observed. Experiments show that the effect of the depth h on the heat transfer is insignificant for heat fluxes far from critical. The right-hand side of Eq. (19) also does not depend on h for $m \gg 1$. It should be noted that in calculating λ_l , following the recommendation of [5], we have assumed that λ_l is proportional to $h^{1/3}$. Thus, in Eq. (19) the heat flux is, in fact, proportional to $h^{1/6}$, i.e., the effect of h is very small. On approaching the critical region, the term $m/(m+1)$ begins to play an appreciable role in Eq. (19). The effect of h becomes significant, which is confirmed by experiment.

In the region of the critical point, the model gives only qualitative agreement with experiment. As ΔT increases, the value of m falls and the curve $q(\Delta T)$ falls beneath the straight-line dependence. This trend corresponds to the physical picture of the phenomenon, since increase in ΔT is associated with increase in resistance, and also hydrodynamic closing, of the channels in the porous layer. However, the quantitative results for the critical heat fluxes that are given by differentiation of Eq. (19) are unsatisfactory. The critical heat fluxes and temperature dependences are much too high. This implies that the resistance assigned to the vapor-generating channels in constructing the model was too low. However, taking into account the complexity of the considered process and also the known inaccuracy following from the assumptions made, the agreement of Eq. (19) with experimental results should be regarded as adequate. This indicates that, in broad outline, the mechanism assumed in the analysis of the process is correct.

NOTATION

T , temperature; ΔT , temperature difference; ΔP , pressure difference; Q , heat flux; q , heat-flux density; G , mass flow rate; λ , thermal conductivity; μ , dynamic viscosity coefficient; ρ , density; r , specific heat of vaporization; θ , angle of wetting; σ , surface-tension coefficient; d , granule diameter; h , δ , linear dimensions. Indices: c , capillary; l , layer; L , liquid; V , vapor; s , saturation; b , base.

LITERATURE CITED

1. Ferrell and Johnson, in: Thermal Tubes [Russian translation], Mir (1972), p. 9.
2. Ferrell and Ollivitch, in: Thermal Tubes [Russian translation], Mir (1972), p. 118.
3. M. I. Berman and Z. R. Gorbis, Teploenergetika, No. 11 (1973).
4. R. Martin, Inzhener-Neftyanik, No. 5 (1970).
5. Chan and Tien, Proceedings of the American Society of Mechanical Engineers, Series C. Heat Transfer [Russian translation], No. 3 (1973), p. 14.

6. W. M. Kays, *Convective Heat and Mass Transfer*, McGraw-Hill, New York (1966).
7. A. V. Lykov, *Transfer Phenomena in Capillary Bodies* [in Russian], GITTL, Moscow (1954).
8. C. O. Bennett and J. E. Myers, *Momentum, Heat and Mass Transfer*, McGraw-Hill, New York (1962).
9. *Nonsteady Heat Transfer* [in Russian], Mashinostroenie (1973).
10. P. J. Schneider, *Conduction Heat Transfer*, Addison-Wesley, Reading, Massachusetts (1955).
11. P. S. O'Neill, C. F. Gottzman, and J. W. Terbot, *Adv. Cryogenic Eng.*, 17 (1972).
12. P. M. Milton and C. F. Gottzman, *Chem. Eng. Progr.*, 68, No. 9 (1972).

NATURAL THERMAL RADIATION OF HEAT-
 ABSORBING THERMAL VACUUM CHAMBER
 SHIELDS

Yu. V. Svetlov, S. P. Gorbachev,
 A. I. Skovorodkin, and R. A. Shagiakhmetov

UDC 536.3

A simplified method for computing the natural thermal radiation of heat-absorbing shields of vacuum chambers is elucidated; computational dependences are presented for shields of herringbone outlines and the influence of the geometric profile characteristics on the magnitude of the natural radiation is shown.

The efficiency of the heat-absorbing shield of a thermal vacuum chamber within which is a radiant energy source depends greatly on how small the radiant flux, going into the chamber from the shield is. This flux consists of two components: the reflected radiant flux and the natural thermal radiation of the shield. It is expedient to examine these components separately for a detailed investigation of the influence of the shield on the radiant heat exchange.

In order to assure the requisite absorptivity of the radiant flux, the shields of thermal vacuum chambers are ordinarily set up in the form of a cellular construction. Each individual cell of the shield is a spatial cavity formed either by adjacent shield profiles or by several surfaces of one profile (Fig. 1a).

In the general case, the magnitude of the natural thermal radiation of a cell in the shield is determined by computing the complex (radiant and conductive) heat exchange on the basis of zonal methods, for example, [2, 3]. As a rule, an awkward iteration method of computation is hence used, since the temperature field in

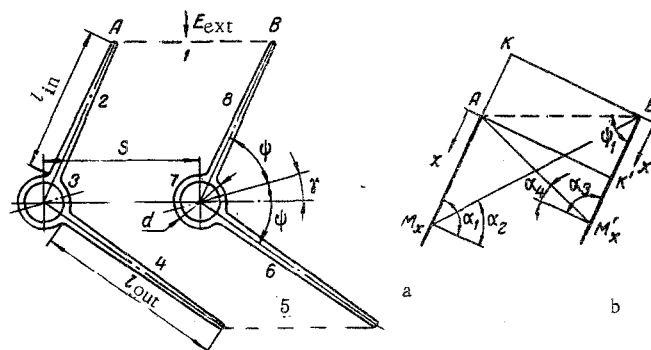


Fig. 1. Cell of a heat-absorbing shield of herringbone profile (a) and analysis of the local angular radiation coefficients from the inner fins of the profile (b).

Translated from *Inzhenerno-Fizicheskii Zhurnal*, Vol. 30, No. 2, pp. 317-321, February, 1976. Original article submitted February 25, 1975.

This material is protected by copyright registered in the name of Plenum Publishing Corporation, 227 West 17th Street, New York, N.Y. 10011. No part of this publication may be reproduced, stored in a retrieval system, or transmitted, in any form or by any means, electronic, mechanical, photocopying, microfilming, recording or otherwise, without written permission of the publisher. A copy of this article is available from the publisher for \$7.50.